JOURNAL OF BACTERIOLOGY, Sept. 2003, p. 5546–5554 Vol. 185, No. 18
0021-9193/03/$08.00+0 DOI: 10.1128/JB.185.18.5546–5554.2003

Interactions of FliJ with the *Salmonella* Type III Flagellar Export Apparatus

Gillian M. Fraser,[1]† Bertha González-Pedrajo,[1] Jeremy R. H. Tame,[2]‡ and Robert M. Macnab[1]*

Department of Molecular Biophysics and Biochemistry, Yale University, New Haven, Connecticut 06520-8114,[1] *and Protonic Nanomachine Project, ERATO, JST, 1-7 Hikaridai, Seika, Kyoto, 619-0237 Japan*[2]

Received 20 May 2003/Accepted 2 July 2003

FliJ, a 17-kDa protein, is a soluble component of the *Salmonella* type III flagellar protein export system that has antiaggregation properties and several other characteristics that suggest it may have a chaperone-like function. We have now examined this protein in detail. Ten-amino-acid scanning deletions covering the entire 147-amino-acid sequence were tested for complementation of a *fliJ* null strain; only the first and last deletions complemented. A few of the deletions, especially towards the C terminus, exerted a dominant negative effect on wild-type cells, indicating that they were actively interfering with function. Two truncated versions of FliJ, representing its N- and C-terminal halves, failed to complement and were not dominant. We tested for FliJ self-association by several techniques. Size-exclusion chromatography (Superdex 200) indicated an apparent molecular mass of around 50 kDa, which could reflect either multimerization or an elongated shape or both. Multiangle light scattering gave a peak value of 20 kDa, close to the molecular mass of the monomer. Analytical ultracentrifugation gave evidence for weak self-association as a trimer or tetramer. It was known from previous studies that FliJ interacts with the N-terminal region of FliH, a negative regulator of the ATPase FliI. Using both truncation and deletion versions of FliJ, we now show that it is its C-terminal region that is responsible for this interaction. We also show that FliJ interacts with the soluble cytoplasmic domain of the largest membrane component of the export apparatus, FlhA; although small deletions in FliJ did not interfere with the association, both truncated versions failed to associate, indicating that a substantial amount of the central region of the FliJ sequence participates in the association. We present a model summarizing these multiple interactions.

Flagellar protein export occurs by a type III pathway. The physical apparatus consists of both integral membrane and soluble components. In addition to some specific chaperones, there are three known soluble components that are necessary for the export of all substrates. Two of these have relatively well-defined functions: FliI is an ATPase whose enzymatic activity is necessary to drive the export process (3, 5, 19), and FliH is a negative regulator of FliI (6, 10, 11, 13) which is thought to prevent futile ATP hydrolysis unlinked to protein translocation.

The third soluble component is FliJ, which is a small 147-residue protein with a deduced molecular mass of 17 kDa, a high proportion (31 mol%) of charged residues, and a high α-helical propensity (19). These are characteristics possessed by many type III export chaperones (2). It also has a region near the N terminus (residues 14 through 42) with an extremely high predicted probability (>80% [8]) of engaging in an α-helical coiled-coil interaction with another FliJ subunit or other proteins with similar predicted properties (see Fig. 1A); of the 80% total probability, approximately 70% is predicted for a coiled-coil dimer and 10% for a trimer. In a previous study (12), we obtained evidence from affinity blotting that FliJ interacts with export substrates, but the signal level was not high. The most convincing evidence that FliJ interacts with export substrates is an indirect one, namely, that it prevents their aggregation (8).

In a recent detailed analysis of FliH, it was shown that not only does it form a complex with FliI, as had been described previously (11), but also it binds to FliJ (6). In the present study we analyze FliJ in more detail, with an emphasis on identifying the regions that are essential for its function and for interaction with other flagellar export components.

MATERIALS AND METHODS

Bacterial strains, plasmids, and media. The strains and plasmids used in this study are listed in Table 1. Luria-Bertani broth (LB) and soft tryptone agar plates were prepared as described previously (12). Ampicillin was added to the media to a final concentration of 100 μg ml^{-1}.

DNA manipulations. Procedures for DNA manipulation in vitro were carried out as described previously (6). PCR was carried out using *PfuTurbo* DNA polymerase (Stratagene). DNA sequencing was carried out with the modified T7 DNA polymerase Sequenase (U.S. Biochemical Corp.). Restriction enzymes and T4 DNA ligase (New England Biolabs) were used according to the manufacturers' instructions.

Construction of FliJ scanning deletion and truncation mutants. *fliJ* deletion mutants were generated using the protocol developed by Toker et al. (18). Wild-type, truncation, and deletion versions of *fliJ* were cloned into pET-based and pTrc99A-FF4-based plasmids (14) using *Nde*I/*Bam*HI and *Xba*I/*Hin*dIII restriction sites, respectively, that were engineered into the PCR primers. All clones were sequenced to verify that no errors had been introduced by the PCR amplification. pTrc99A-based plasmids cooverproducing His-FliJ or its deletion/

* Corresponding author. Mailing address: Department of Molecular Biophysics and Biochemistry 0734, Yale University, P.O. Box 208114, 266 Whitney Ave., New Haven, CT 06520-8114. Phone: (203) 432-5590. Fax: (203) 432-9782. E-mail: robert.macnab@yale.edu.

† Present address: Department of Pathology, Cambridge University, Cambridge, CB2, 1QP, United Kingdom.

‡ Present address: Yokohama City University, 1-7-29, Suehiro, Tsurumi, Yokohama Kanagawa 230-0045, Japan.

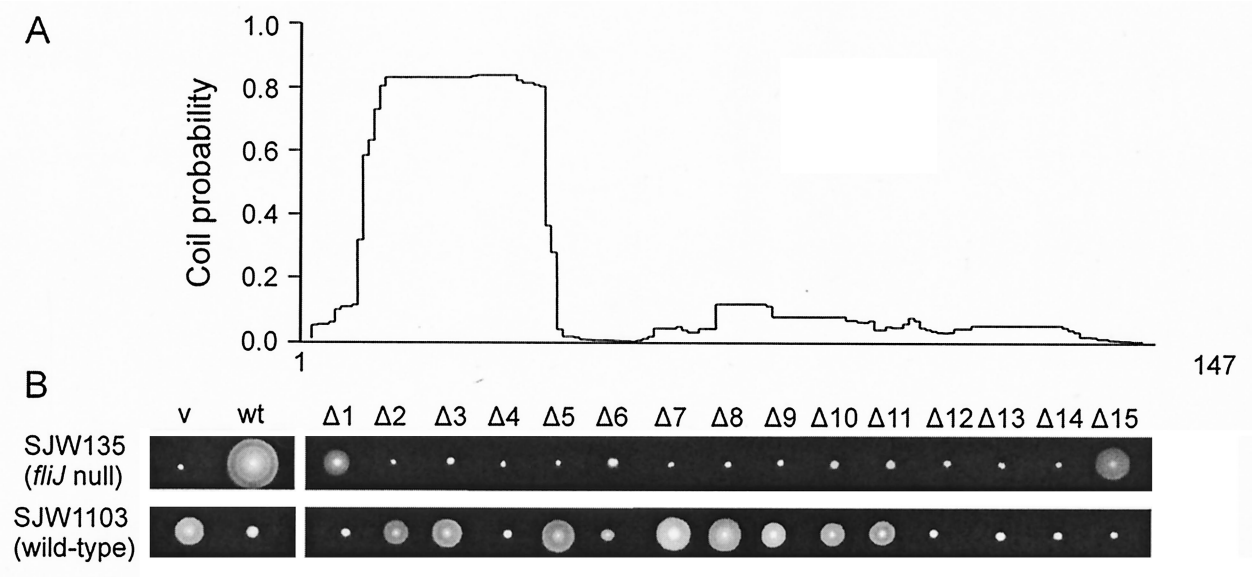

FIG. 1. (A) Probability that a given amino acid of the 147-residue FliJ protein will participate in an α-helical coiled-coil structure, as calculated by the Multicoil program of Wolf et al. (20). Residues 14 through 42 are predicted to have a >80% probability of forming a coiled-coil structure (8). (B, upper panels) Complementation of the motility defect of the *fliJ* mutant strain SJW135 transformed with pTrc99A-FF4-based plasmids encoding various forms of His-tagged FliJ. v, pTrc99A-FF4; wt, wild-type FliJ; Δ1, etc., 10-amino-acid deletion variants of FliJ. Semisolid tryptone agar plates inoculated with the transformants were incubated at 30°C for 6 h. (B, lower panels) Multicopy effects on the motility of wild-type SJW1103 transformed with the same plasmids as described above. Plates were incubated at 30°C for 5 h.

truncation variants with FliH or His-FlhA_C were constructed as described previously (12).

Analysis of motility on soft tryptone agar plates. For complementation studies, freshly transformed SJW135 cells carrying pTrc99A-FF4-based plasmids were inoculated into soft tryptone agar plates containing ampicillin and incubated at 30°C for 6 h. For multicopy and negative dominance effects, plasmids were transformed into SJW1103 cells, inoculated into soft agar plates containing ampicillin and 0.1 mM isopropyl-β-D-thiogalactopyranoside (IPTG), and incubated at 30°C for 5 h.

Overproduction and purification of N-terminally His-tagged proteins. His-tagged proteins were purified from the soluble fractions of either BL21(DE3)pLysS cells carrying pET-based plasmids or SJW1368 Δ(*cheW-flhD*) carrying pTrc-based plasmids by using Ni-iminodiacetic acid (IDA) His-Quick 900 cartridges (Novagen) as described previously (6).

Overproduction and purification of native FliJ. BL21(DE3) cells transformed with pMM408 (a pET-based plasmid encoding untagged FliJ) were grown overnight at 37°C in LB plus 100 μg of ampicillin/ml. Five milliliters of this culture was inoculated into 5 liters of LB plus ampicillin in a 10-liter fermentor and grown at 37°C with stirring for 3 to 4 h until the optical density at 650 nm had reached 0.4. IPTG was added to a final concentration of 0.2 mM, and growth continued for a further 2 h. The cells were harvested, resuspended in 50 ml of buffer A (50 mM HEPES [pH 7], 100 mM NaCl, 1 mM dithiothreitol) plus 1 tablet of Complete protease inhibitor (Boehringer-Mannheim), and frozen at −80°C until needed. The cells were then thawed, sonicated, and centrifuged at 142,400 × *g* for 45 min, and the supernatant was dialyzed against buffer A and recentrifuged. An SP (sulfopropyl) Sepharose 16/10 cation exchange column (Pharmacia) was prepared with buffer A. The sample was loaded, and the column was washed with one volume of buffer A and then subjected to a salt gradient from 100 to 500 mM NaCl using buffer A and buffer B (buffer A plus 1 M NaCl). Fractions containing FliJ with only minor contaminants (as judged by sodium dodecyl sulfate-polyacrylamide gel electrophoresis [SDS-PAGE]) were pooled, the identity of the protein was verified by matrix-assisted laser desorption ionization–time-of-flight spectroscopy, and the sample was used for analytical ultracentrifugation.

Size exclusion chromatography and multiangle light scattering. Purified proteins were dialyzed against 20 mM Tris-HCl (pH 7.4), 150 mM NaCl, 1 mM EDTA, 1 mM dithiothreitol and subjected to size-exclusion chromatography on a Superdex 200 HR 10/30 column (Pharmacia) using a Biologic System (Bio-Rad). Thyroglobulin (669 kDa), ferritin (440 kDa), catalase (232 kDa), aldolase (158 kDa), bovine serum albumin (67 kDa), ovalbumin (43 kDa), chymotrypsinogen A (25 kDa), and RNase A (13.7 kDa) were used as molecular mass markers. Size exclusion chromatography (Superdex 75 HR 10/30; Pharmacia) followed by in-line multiangle light scattering (Waters 996 Photodiode Array-PDA detector; DAWN-DSP and Optilab DSP; Wyatt Technology) was carried out at the Keck Foundation Biotechnology Resource Laboratory, Yale University.

Analytical ultracentrifugation. Sedimentation equilibrium experiments were carried out using a Beckman Optima XL-A analytical ultracentrifuge with an AnTi 60 rotor. Data were obtained at 20°C at four different speeds (10, 12, 18, and 28 krpm) and two concentrations, with initial A_{280} values of 0.25 and 0.5 (equivalent to about 9 and 18 μM, respectively). The samples were extensively dialyzed against the buffer (50 mM Tris-HCl [pH 8.0]), which was also used as a blank. All measurements were made at a wavelength of 280 nm. The data were analyzed with the manufacturer's software. Solvent density and partial specific volumes were calculated from standard tables using the program SEDNTERP (7).

Affinity blotting. Affinity blotting of His-FliJ variants with His-FLAG-tagged FliH and FlhA_C probes was carried out as previously described (12). Detection was performed with an ECL detection kit (Amersham).

Ni-IDA affinity chromatography copurification (pull-down) assays. His-FliJ or its deletion/truncation variants were cooverproduced with untagged FliH in SJW1368, and proteins were copurified by affinity chromatography on Ni-IDA His-Quick 900 cartridges as described previously (6).

RESULTS

Complementation and dominance properties of deletion and truncation variants of FliJ. We constructed a set of pTrc-based plasmids encoding 15 scanning deletion variants of N-terminally His-tagged FliJ (His-FliJΔ1, FliJΔ2, etc.). Each deletion was of 10 amino acids except for the last one (His-FliJΔ15), which extended from residue 141 to the C terminus (residue 147). All of the deletion variants were expressed at similar levels (data not shown). We also constructed two truncated versions of N-terminally His-tagged FliJ, an N-terminal one containing residues 1 to 73 [His-FliJ(1-73)] and a C-terminal one containing residues 74 to 147 [His-FliJ(74-147)].

TABLE 1. Strains and plasmids used in this study

Strain or plasmid	Relevant characteristic(s)	Source or reference
E. coli strains		
NovaBlue	Recipient for cloning experiments	Novagen
BL21(DE3) and BL21(DE3)pLysS	For overproduction of proteins from pET-based plasmids	Novagen
Salmonella strains		
JR501	$r^- m^+$; for converting plasmids to *Salmonella* compatibility	16
SJW1103	Wild type for motility and chemotaxis	21
SJW1368	Δ(*cheW-flhD*); master operon mutant	15
SJW135	*fliJ* mutant	8
Plasmids		
pTrc99A	pTrc expression vector	Pharmacia
pTrc99A-FF4	pTrc expression vector	14
pET19b	N-terminally His-tagged pT7 expression vector	Novagen
pMM408	pET22b FliJ	12
pMM406	pTrc99A His-FliJ	12
pMM308	pET19b His-FLAG-FliH	12
pGF406iH	pTrc99A His-FliJ + FliH	6
pMM102	pTrc99A His-$FlhA_C$	12
pMM103	pTrc99A His-FLAG-$FlhA_C$	12
pMM102J	pTrc99A His-$FlhA_C$ + His-FliJ	12
pGFJΔ1, pGFJΔ2, etc., to pGFJΔ15	pET19b His-FliJΔ(1–10), His-FliJΔ(11–20), etc., to His-FliJΔ(141–147)	This study
pGFTJΔ1, pGFTJΔ2, etc., to pGFTJΔ15	pTrc99A-FF4 His-FliJΔ(1–10), His-FliJΔ(11–20), etc., to His-FliJΔ(141–147)	This study
pGFJ1-73	pET19b His-FliJ(1–73)	This study
pGFJ74–147	pET19b His-FliJ(74–147)	This study
pGFTJ1–73	pTrc99A-FF4 His-FliJ(1–73)	This study
pGFTJ74–147	pTrc99A-FF4 His-FliJ(74–147)	This study
pGFTJ1–73iH	pTrc99A His-FliJ(1–73) + FliH	This study
pGFTJ74–147iH	pTrc99A His-FliJ(74–147) + FliH	This study
pGFTJΔ9iH, etc., to pGFTJΔ15iH	pTrc99A His-FliJΔ9, etc., to His-FliJΔ15 + FliH	This study

The choice of the latter fragments was based on a mutant, SJW277, which has an amber codon at position 74 and played a prominent role in a previous study (8).

The results of motility complementation tests in soft agar, using the null mutant SJW135 (which encodes only the first 14 amino acids of FliJ [8]), are shown in the upper panel of Fig. 1B. The two terminal deletion variants (His-FliJΔ1 and His-FliJΔ15) complemented fairly well, His-FliJΔ11 through His-FliJΔ13 complemented poorly after prolonged incubation (data not shown), and the remaining variants (His-FliJΔ2 through His-FliJΔ10, and also His-FliJΔ14) did not complement at all. Thus, it appears that almost all of the FliJ sequence is essential for function.

When the plasmids were induced with 0.1 mM IPTG, those that had complemented (including the one expressing wild-type *fliJ*) showed reduced complementation (data not shown), a well-established negative multicopy effect of FliJ (12).

When the wild-type strain SJW1103 was transformed with the *fliJ* deletion plasmids and the cells were induced with 0.1 mM IPTG (Fig. 1B, lower panel), those that had complemented the SJW135 mutant, with the exception of that encoding His-FliJΔ11, showed a negative multicopy effect. Motility was also reduced in cells producing His-FliJΔ4, His-FliJΔ6, and His-FliJΔ14, suggesting that these noncomplementing deletion variants exert negative dominance. The remaining FliJ variants had no effect on wild-type motility, i.e., there was no multicopy effect or negative dominance.

The FliJ truncates His-FliJ(1-73) and His-FliJ(74-147) failed to complement and had no negative multicopy effect on wild-type motility (data not shown). Plasmids encoding untagged FliJ(1-73) or FliJ(1-73)-His also failed to complement (data not shown). In contrast, strain SJW277, with an amber codon at position 74, had previously been found to be significantly more motile than other *fliJ* mutants, and a plasmid carrying the *fliJ277* allele expressed under inducing conditions gave almost complete complementation (8). We introduced a deletion into pMM410 (the plasmid carrying the *fliJ277* allele) that disrupted the *fliJ* coding sequence downstream of the amber stop codon but left codons 1 to 74 intact. This deletion version of pMM410 failed to complement the *fliJ* null mutant (data not shown). In the Discussion section, we will return to the apparent discrepancy between the results with FliJ277 and His-FliJ(1-73).

Self-association properties of FliJ. The predicted coiled-coil at the N terminus of FliJ (8) (Fig. 1A) suggested to us that this region might promote FliJ-FliJ interaction. We therefore sought evidence for FliJ oligomerization using size-exclusion chromatography, multiangle light scattering, and sedimentation equilibrium analytical ultracentrifugation (AUC).

When subjected to size exclusion chromatography using a Superdex 200 HR 10/30 column, His-FliJ eluted at a position corresponding to an apparent molecular mass of around 50 kDa (Fig. 2A), suggesting that, if the molecule was close to spherical, it was eluting as a dimer or trimer. The elution profile was unusually broad, indicating that it may have been polydisperse. His-FliJ was further analyzed by size exclusion

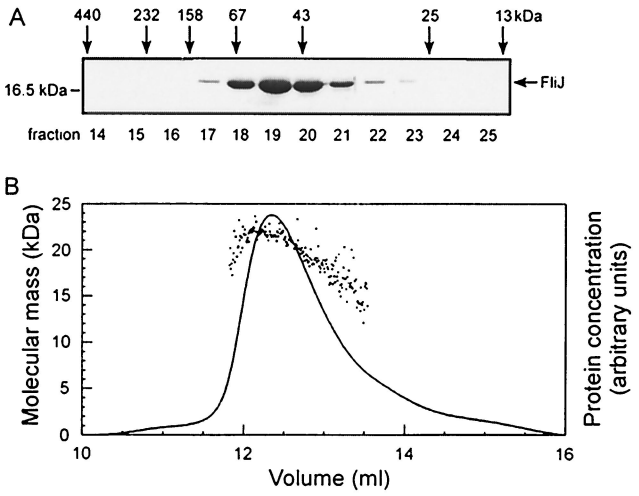

FIG. 2. (A) Size-exclusion chromatography of purified His-FliJ on a Superdex 200 HR 10/30 column. Elution fractions (14 to 25) were analyzed by SDS-PAGE (15% acrylamide) and stained with Coomassie brilliant blue. The His-FliJ elution profile is unusually broad and asymmmetric, peaking at a molecular mass of approximately 50 kDa. Vertical arrows indicate elution positions of molecular mass markers. (B) Size exclusion chromatography (Superdex 75 HR 10/30) and in-line multiangle light scattering analysis of purified His-FliJ. The elution profile of His-FliJ is shown as a solid line (right axis label), and clustered points represent light-scattering data converted to molecular mass (left axis label). The average molecular mass of eluted His-FliJ, as determined by multiangle light scattering, is approximately 20 kDa.

chromatography on a Superdex 75 HR 10/30 column followed by in-line multiangle light scattering, a technique which determines the mass of a molecule independently of its shape. In this case, His-FliJ eluted from the column at a position corresponding to a molecular mass of about 29 kDa and, as with the Superdex 200 column, the elution peak was unusually broad (Fig. 2B). The multiangle light scattering signal peaked at around 22 kDa but trailed considerably down to a value of around 16 kDa and with an average molecular mass of 20.1 kDa, consistent with the calculated mass of 20 kDa for the His-FliJ monomer.

To further examine the possibility of FliJ oligomerization, we performed sedimentation equilibrium AUC of the purified untagged protein. Like multiangle light scattering, sedimentation equilibrium AUC determines molecular mass independently of shape. The manufacturer's software was used to test several models (Fig. 3). A simple monomeric model produced a poor fit both in terms of high residuals and an estimated molecular mass of 32.2 kDa that was much higher than the actual value of 17.3 kDa. When the molecular mass was constrained to its actual value, the fit was even worse. Fit to a monomer-dimer equilibrium was poor. A monomer-trimer fit was good, and a monomer-tetramer fit produced no further improvement. Using the monomer-trimer model, for which an association constant of $4.1 \times 10^9\ M^{-2}$ was predicted by the software, and a total protein concentration of 10 μM (expressed as monomer equivalents), we calculated that in uniform solution the monomer-trimer ratio (again expressed as monomer equivalents) is about 1:0.5. Thus, while the data provide evidence for FliJ trimerization, they do not suggest a very tight association. This is consistent with the multiangle light scattering signal result, which indicates that the peak fraction was predominantly monomeric. In parallel to the analysis of FliJ, we also ran sedimentation equilibrium experiments with purified His-FliJΔ2, His-FliJΔ3, and His-FliJΔ4, which contain 10-amino-acid deletions in the putative coiled-coil region. As with native FliJ, the data obtained from analysis of these deletion variants were best fitted to a monomer-trimer model (data not shown).

FliJ-FliH interactions. FliH is a negative regulator of the flagellar ATPase FliI (11). A recent study demonstrated by Ni-affinity chromatography that FliJ interacts with FliH, primarily its N-terminal region (6). To determine which regions of FliJ are responsible for this interaction, we used two approaches: Ni-affinity chromatography and affinity blotting. Initially, we examined the interaction of FliH with the two FliJ truncation variants, His-FliJ(1-73) and His-FliJ(74-147) (Fig. 4). Untagged FliH was coproduced with His-FliJ, His-FliJ(1-73), or His-FliJ(74-147) in the nonflagellate SJW1368 Δ(*cheW- flhD*) mutant, and soluble cell lysates were passed down an Ni-IDA column. After extensive washing, bound proteins were eluted from the column and analyzed by SDS-PAGE (Fig. 4A). As expected from previous work (6), FliH was retained on the column by His-FliJ. It was also retained by the His-FliJ(74-147) truncate, which lacks the N-terminal 73 amino acids of FliJ, but not by His-FliJ(1-73), indicating that it is the C-terminal half of FliJ that interacts with FliH. This result was confirmed by affinity blotting of His-FliJ and the truncates with a His-FLAG-FliH probe (Fig. 4B), which bound to full-length His-FliJ and His-FliJ(74-147) but very weakly if at all to His-FliJ(1-73).

To define more precisely the region within the C-terminal domain of FliJ that is involved in the interaction with FliH, we carried out Ni-affinity chromatography and affinity blot experiments with His-FliJ variants containing consecutive 10-amino-acid deletions between residues 81 and 147, i.e., His-FliJΔ9 through His-FliJΔ15 (Fig. 5). Ni-affinity chromatography showed that 10-amino-acid deletions between residues 81 and 110 (His-FliJΔ9, His-FliJΔ10, and His-FliJΔ11) and between 131 and 147 (His-FliJΔ14 and His-FliJΔ15) weakened the interaction with FliH (Fig. 5A), and affinity blotting indicated that deletion of residues 101 to 110 (His-FliJΔ11) had a particularly severe effect (Fig. 5B). The reason why His-FliJΔ15 appeared as a doublet is unknown but may indicate degradation.

Interaction of FliJ with $FlhA_C$. FlhA is the largest component of the export apparatus, with a molecular mass of 75 kDa. It is an integral membrane protein and has a C-terminal cytosolic domain, $FlhA_C$, that could be a possible docking target for the soluble components of the export system, including FliJ. Indeed, an interaction between FliJ (as target) and $FlhA_C$ (as probe) was identified during an affinity blot analysis of export component interactions (12). We further examined this interaction using size-exclusion chromatography. As described above, His-FliJ elutes from a Superdex 200 size-exclusion column at around 50 kDa. N-His-$FlhA_C$, which has a molecular mass of about 40 kDa, elutes at approximately the same position as the 67-kDa molecular mass marker (Fig. 6), suggesting it has a somewhat elongated shape and perhaps also, as FRET data indicate (22), is self-associating to some degree. When copurified His-FliJ and His-$FlhA_C$ were applied to the column,

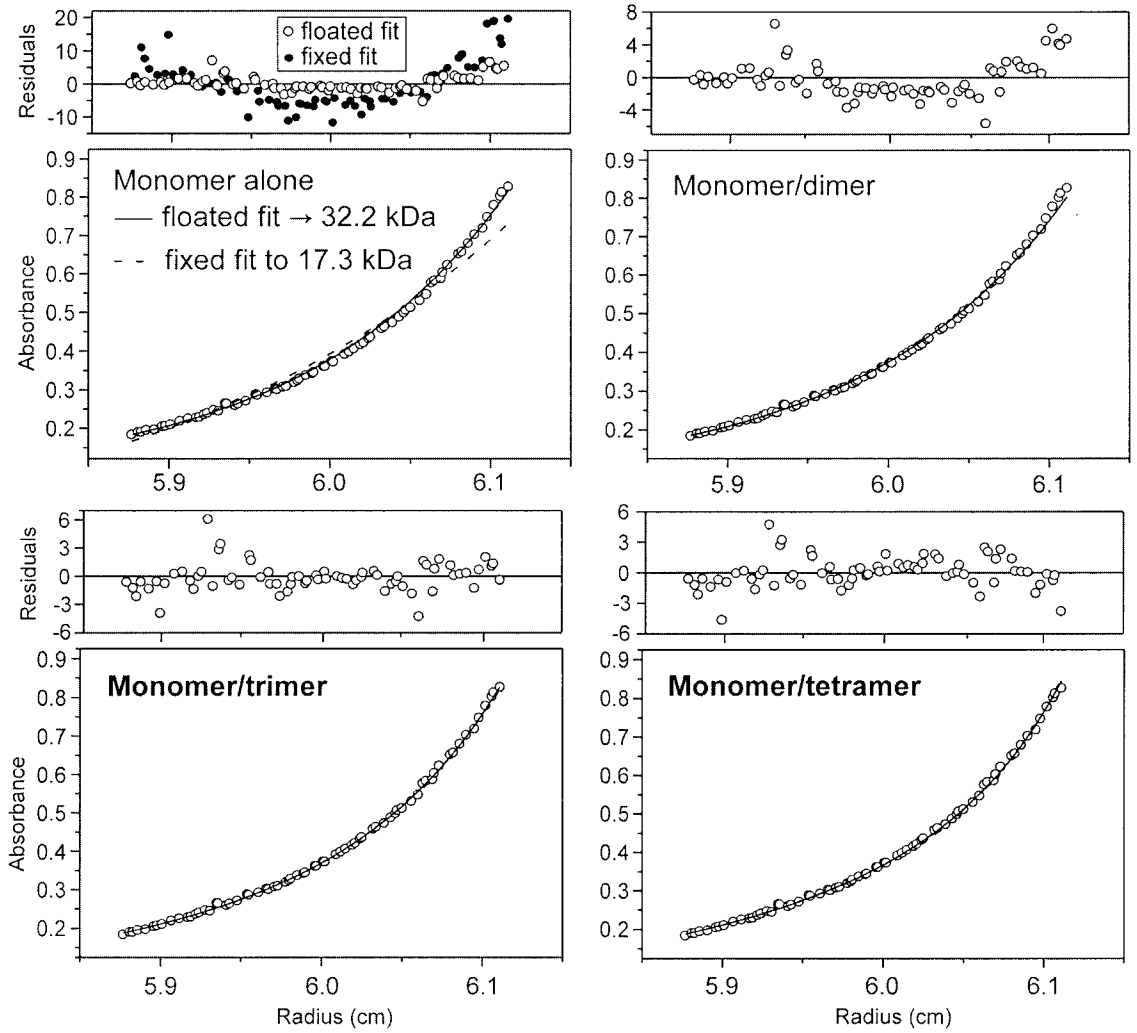

FIG. 3. Sedimentation equilibrium AUC analysis of untagged FliJ. Data points are fitted to various models as follows: top left, FliJ monomer (with either a fixed fit to the known monomeric mass of 17.3 kDa [solid circles] or a floated fit [open circles]); top right, monomer-dimer equilibrium; bottom left, monomer-trimer equilibrium; bottom right, monomer-tetramer equilibrium. Note that the scales for the residuals are not the same for all panels.

they comigrated with a peak position at around 150 kDa. We conclude that they form a stable FliJ-FlhA_C complex.

Next, we attempted to identify the region of FliJ involved in the interaction with FlhA_C by affinity blotting full-length His-FliJ, His-Fli(J1-73), and His-FliJ(74-147) with a His-FLAG-FlhA_C probe (Fig. 7). His-FLAG-FlhA_C recognized full-length His-FliJ but did not bind to either of the truncates, suggesting that elements of both regions are required for the interaction. We carried out similar affinity blotting with the His-FliJ 10-amino-acid deletion variants, but all were recognized by His-FLAG-FlhA_C (data not shown).

DISCUSSION

FliJ is central to the efficient type III export of flagellar structural proteins. In previous studies, it was shown by affinity blotting that FliJ was recognized, albeit weakly, by flagellar export substrates and that it functioned in vivo like a chaperone, preventing aggregation of substrates in the cytoplasm (8, 12). It has also been shown that FliJ interacts with other components of the flagellar export apparatus (6, 12).

In this study, we have analyzed FliJ in detail, focusing particularly on its interactions with other export components. We have determined which regions of FliJ are required for full function, provided evidence that FliJ can oligomerize in vitro, and shown that the C-terminal half of FliJ interacts with FliH, the regulator of the flagellar export ATPase FliI. We have also shown that FliJ forms a complex with the cytosolic domain of FlhA, an integral membrane component of the export apparatus.

FliJ is generally intolerant of 10-amino-acid deletions. Of the 15 FliJ deletion variants that we constructed all, except those with deletions at the extreme N and C termini, either abolished or severely attenuated FliJ function. We also tested whether overproduction of the deletion variants had a negative multicopy effect on wild-type motility, as occurs with wild-type FliJ (8). His-FliJΔ4, His-FliJΔ6, and His-FliJΔ14 were dominant negative, suggesting that they might be able to interact

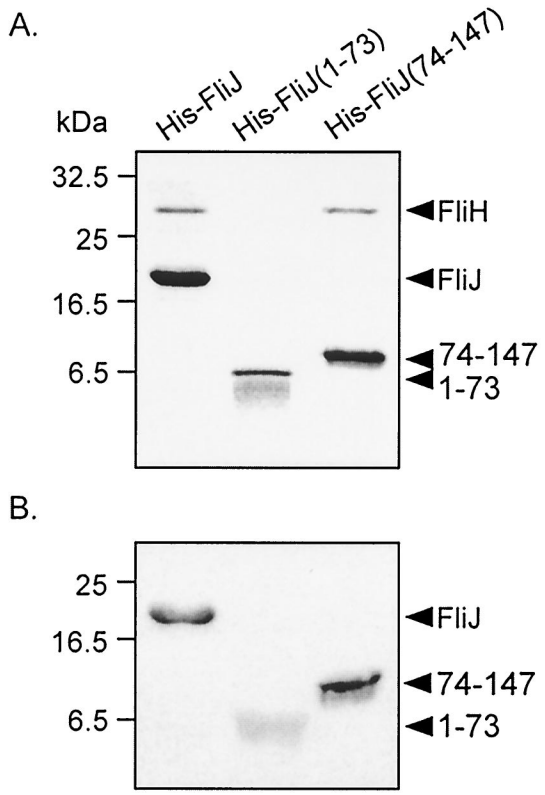

FIG. 4. Interactions of FliJ truncates with FliH. (A) Affinity chromatography copurification assays. His-tagged FliJ or its truncation derivatives His-FliJ(1-73) (comprising the N-terminal 73 residues of FliJ) and His-FliJ(74-147) (comprising its C-terminal 74 residues) were coproduced with untagged FliH and subjected to Ni-affinity chromatography. Eluted proteins were separated by SDS-PAGE and visualized by staining with Coomassie brilliant blue. FliH copurifies with full-length His-FliJ and His-FliJ(74-147), but not with His-FliJ(1-73). Molecular mass markers are shown to the left. (B) Affinity blotting. His-FliJ, His-FliJ(1-73), and His-FliJ(74-147) were subjected to SDS-PAGE, transferred to nitrocellulose, and incubated with a His-FLAG-FliH probe. Bound His-FLAG-FliH was detected by immunoblotting with anti-FLAG antibody.

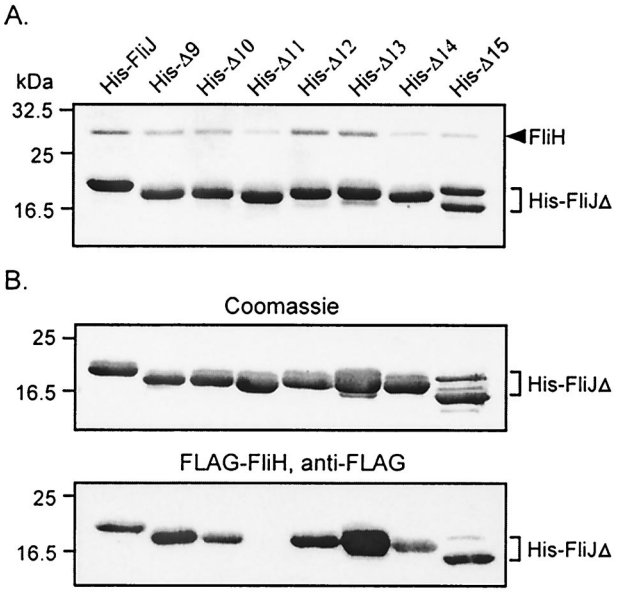

FIG. 5. Interactions of FliJ deletion variants with FliH. (A) Affinity chromatography copurification assays. His-tagged FliJ or its deletion derivatives His-FliJΔ9, etc. (abbreviated as His-Δ9, etc.) were coproduced with untagged FliH and subjected to Ni-affinity chromatography. Eluted proteins were separated by SDS-PAGE and visualized by staining with Coomassie brilliant blue. The His-FliJ(1-73) lane of Fig. 4A provides a negative control where no interaction with FliH was observed. (B) Affinity blotting. His-FliJ and its deletion derivatives were subjected to SDS-PAGE and either visualized by staining with Coomassie brilliant blue (upper panel) or transferred to nitrocellulose and incubated with a His-FLAG-FliH probe (lower panel). Bound His-FLAG-FliH was detected by immunoblotting with anti-FLAG antibody. It is not clear why His-FliJΔ15 appears as a doublet.

with other flagellar components, e.g., FliJ, FliH, or $FlhA_C$, and sequester them into nonfunctional complexes that impede the export process. Overproduction of all but one of the functional or partially functional deletion variants, like wild-type FliJ, produced a negative multicopy effect. The exception was His-FliJΔ11; it may be significant that this variant is severely reduced in its ability to bind to FliH, as is discussed below.

A true FliJ(1-73) truncate is not functional. In a previous study, it was found that overexpression of a *fliJ* mutant allele, *fliJ277*, with an amber (TAG) stop codon at position 74 could complement the motility defect of a *fliJ* null mutant, especially if the gene was overexpressed, and the FliJ277 truncate was the only product detected by immunoblotting (8). From these results it was concluded, reasonably, that the N-terminal 73 residues of FliJ were sufficient to provide full function. This would seem contradictory to the scanning deletion analysis in the present study, which indicated that essentially all of FliJ was necessary for function, and prompted us to reexamine the issue of the dispensability of the C-terminal region of FliJ. To do so, we constructed a truncated variant of *fliJ* with an ochre (TAA) stop codon at position 74 and no *fliJ* coding sequence beyond that point. We found that this truncate did not complement the *fliJ* null mutant, even though the truncated His-FliJ(1-73) protein was being produced and was soluble and stable. This result and the results with several other constructs suggest that the interpretation of the previously published data was incorrect and that the complementation by *fliJ277* is a consequence of low-level read-through of the amber stop codon, generating full-length FliJ. This would suggest, incidentally, that quite low levels of FliJ suffice to sustain function, although we have not established this directly. We conclude that the C-terminal region of FliJ is indeed essential for function.

FliJ shows weak oligomerization in vitro. Residues 14 to 42 in the N-terminal region of FliJ are strongly predicted to form a coiled-coil structure (Fig. 1), and it has been suggested that this region might be an interface for FliJ oligomerization (8). Indeed, secondary structure and coiled-coil predictions for FliJ are very similar to those for the bacterial histone-like protein H-NS, which dimerizes via a coiled-coil structure in its N-terminal region (4, 17). We investigated the possibility of FliJ oligomerization using size-exclusion chromatography and multiangle light scattering and found that FliJ elutes from a Superdex 200 column with an apparent molecular mass of 50 kDa, suggesting formation of a dimer or trimer, but elutes from a Superdex 75 column with a much smaller mass of 29 kDa; the reason for the different apparent molecular masses is under investigation. Multiangle light scattering analysis (in-line

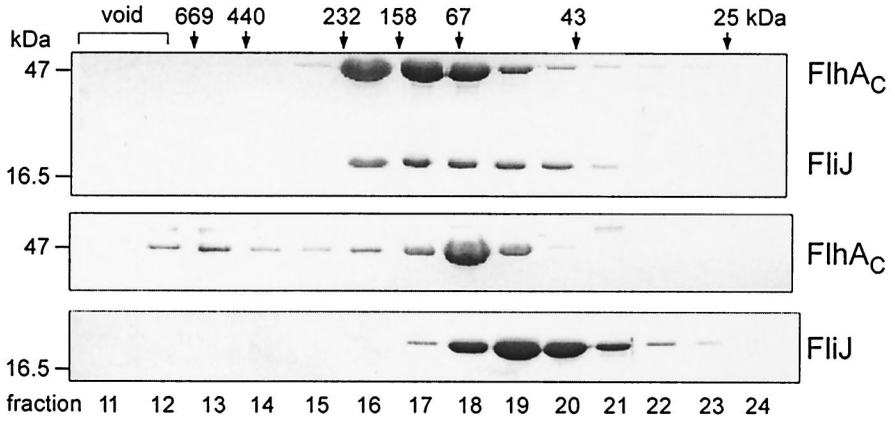

FIG. 6. Size-exclusion chromatography on a Superdex 200 HR 10/30 column of the His-FliJ/His-FlhA$_C$ complex (top panel), His-FlhA$_C$ (middle panel), and His-FliJ (bottom panel). Elution fractions (11 to 24) were analyzed by SDS-PAGE (15%), and proteins were visualized by staining with Coomassie brilliant blue. Vertical arrows indicate elution positions of molecular mass markers.

with the Superdex 75 column) indicated that FliJ was predominantly monomeric; however, the broad polydisperse elution peak suggests some oligomerization of the monomer during chromatography. Analysis by sedimentation equilibrium AUC confirmed that FliJ could form trimers (or possibly tetramers), although this self-association does not appear to be tight. AUC analysis of FliJ variants that contained 10-amino-acid deletions within the N-terminal predicted coiled-coil region produced data similar to those obtained with wild-type FliJ, suggesting that either these deletions are too small to disrupt oligomerization or that the coiled-coil region is not the oligomerization interface. We constructed a FliJ variant with a deletion spanning the predicted coiled-coil, but it formed aggregates and was not suitable for AUC analysis.

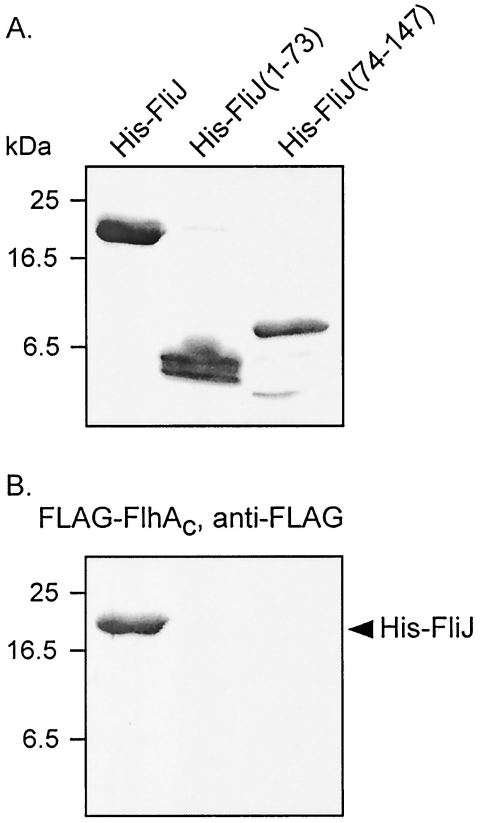

FIG. 7. His-FliJ and its truncation variants His-FliJ(1-73) and His-FliJ(74-147) were subjected to SDS-PAGE and either visualized by staining with Coomassie brilliant blue (A) or transferred to nitrocellulose and incubated with a His-FLAG-FlhA$_C$ probe (B). Bound His-FLAG-FlhA$_C$ was detected by immunoblotting with anti-FLAG antibody.

It is interesting that the nonfunctional truncation and deletion mutants of FliJ were generally not dominant, suggesting that these proteins were not forming hybrid oligomers with wild-type FliJ.

The C-terminal 74 residues of FliJ are sufficient for its interaction with FliH. FliJ interacts with FliH, the regulator of the flagellar export ATPase, FliI, and when FliJ and FliH are coproduced under noninducing conditions in wild-type *Salmonella* they act synergistically to inhibit motility (6, 12). Previously presented evidence indicated that FliJ binds to the N-terminal regions of a FliH dimer (6), but it was not known which regions of FliJ were involved in the interaction. Here we have shown that the His-FliJ(74-147) truncate, which lacks the N-terminal 73 residues of FliJ, binds to FliH in Ni affinity chromatography assays and affinity blotting, whereas the His-FliJ(1-73) truncate does not. The fact that none of the 10-amino-acid deletions in the C terminus of FliJ completely abolished FliH binding indicates that the interaction interface could be quite extensive. The deletion of residues 101 to 110 (His-FliJΔ11) produced the most severe effect, suggesting that this region forms an important part of the FliH binding site.

FliJ forms a soluble complex with FlhA$_C$ in vitro. There is growing evidence that soluble flagellar export components can associate peripherally with the cytoplasmic membrane, possibly through their interactions with integral membrane export proteins (9, 12, 22) and/or their inherent affinity for phospholipids (1). Here we have shown that FliJ forms a complex with the large cytosolic C-terminal domain of FlhA, suggesting that, at some stage during flagellar biogenesis, FliJ docks at the membrane export apparatus. In our attempts to identify the region of FliJ that directs the interaction with FlhA$_C$, we found

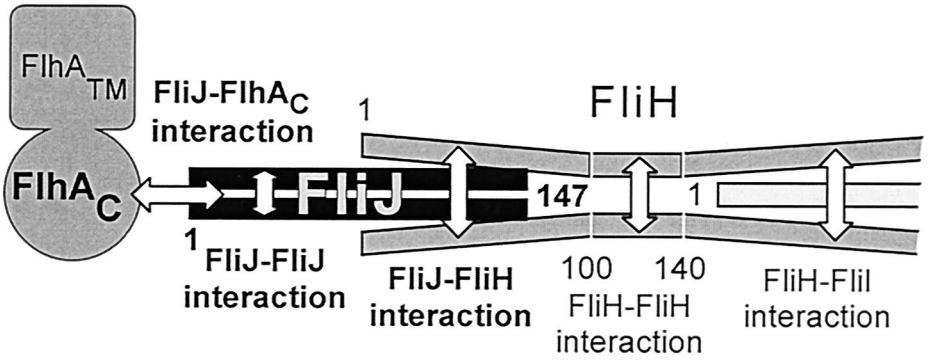

FIG. 8. Schematic illustration of interactions of FliJ (black) and other components of the export system, FliH and the cytosolic C-terminal domain of FlhA, $FlhA_C$ (gray). The transmembrane domain of FlhA is indicated as $FlhA_{TM}$ (gray). Interactions are indicated by double-headed white arrows. FliJ self-associates with a poorly defined stoichiometry (shown here for simplicity as a dimer). Its C-terminal region associates with the N-terminal region of FliH (which itself forms a dimer). FliJ associates with $FlhA_C$, although the precise region(s) of FliJ involved has not been defined. The C terminus of FliH interacts with the N terminus of the ATPase FliI (light gray) (6, 11).

that neither His-FliJ(1-73) nor His-FliJ(74-147) could bind to $FlhA_C$ in affinity blot assays, demonstrating that both of these regions contribute to binding. The FliJ deletion variants all interacted with $FlhA_C$ in affinity blot assays, indicating that, provided most of the FliJ sequence is present, the association is sustained.

A model for FliJ interactions with FliH and $FlhA_C$. A schematic illustration of the principal interactions of FliJ with other components of the export apparatus is given in Fig. 8. FliJ interacts with the soluble domain of FlhA, with the interaction apparently requiring extensive portions of the FliJ sequence, both N terminal and C terminal. A more specific interaction is that between the C-terminal region of FliJ and the N-terminal region of FliH. FliJ oligomerization occurs but it is not a strong association, with different types of assays yielding different results; perhaps the clearest evidence for FliJ self-association is that AUC data could not be fit to a monomer model but gave a good fit to either a monomer-trimer or a monomer-tetramer equilibrium. The interactions continue with the previously established and very stable FliH dimerization via a short domain in the central portion of its sequence and the strong interaction of this homodimer with the type III ATPase, FliI, employing the C-terminal region of FliH and the N-terminal region of FliI (6, 11) but not its catalytic domain. When taken together with interactions which are not presented in Fig. 8 (most notably those with the export substrates themselves, which are still poorly understood), the picture emerges of a large and probably quite dynamic complex which is absolutely essential for flagellar assembly.

ACKNOWLEDGMENTS

We acknowledge Tohru Minamino for assistance with plasmid constructions.

This work has been supported by U.S. Public Health Service grant AI12202, by a Wellcome Trust postdoctoral fellowship (to G.M.F.), and by a postdoctoral fellowship from Consejo Nacional de Ciencia y Tecnología (CONACYT) (to B.G.P.).

REFERENCES

1. **Auvray, F., A. J. Ozin, L. Claret, and C. Hughes.** 2002. Intrinsic membrane targeting of the flagellar export ATPase FliI: interaction with acidic phospholipids and FliH. J. Mol. Biol. **318:**941–950.
2. **Bennett, J. C. Q., and C. Hughes.** 2000. From flagellum assembly to virulence: the extended family of type III export chaperones. Trends Microbiol. **8:**202–204.
3. **Dreyfus, G., A. W. Williams, I. Kawagishi, and R. M. Macnab.** 1993. Genetic and biochemical analysis of *Salmonella typhimurium* FliI, a flagellar protein related to the catalytic subunit of F_0F_1 ATPase and to virulence proteins of mammalian and plant pathogens. J. Bacteriol. **175:**3131–3138.
4. **Esposito, D., A. Petrovic, R. Harris, S. Ono, J. F. Eccleston, A. Mbabaali, I. Haq, C. F. Higgins, J. C. D. Hinton, P. C. Driscoll, and J. E. Ladbury.** 2002. H-NS oligomerization domain structure reveals the mechanism for high order self-association of the intact protein. J. Mol. Biol. **324:**841–850.
5. **Fan, F., and R. M. Macnab.** 1996. Enzymatic characterization of FliI: an ATPase involved in flagellar assembly in *Salmonella typhimurium.* J. Biol. Chem. **271:**31981–31988.
6. **González-Pedrajo, B., G. M. Fraser, T. Minamino, and R. M. Macnab.** 2002. Molecular dissection of *Salmonella* FliH, a regulator of the ATPase FliI and the type III flagellar protein export pathway. Mol. Microbiol. **45:**967–982.
7. **Laue, T. M., B. Shah, T. M. Ridgeway, and S. L. Pelletier.** 1992. Computer-aided interpretation of analytical sedimentation data for proteins, p. 90–125. *In* S. E. Harding, J. C. Horton, and A. J. Rowe (ed.), Analytical ultracentrifugation in biochemistry and polymer science. Royal Society of Chemistry, Cambridge, United Kingdom.
8. **Minamino, T., R. Chu, S. Yamaguchi, and R. M. Macnab.** 2000. Role of FliJ in flagellar protein export in *Salmonella.* J. Bacteriol. **182:**4207–4215.
9. **Minamino, T., B. González-Pedrajo, M. Kihara, K. Namba, and R. M. Macnab.** 2003. The ATPase FliI can interact with the type III flagellar protein export apparatus in the absence of its regulator FliH. J. Bacteriol. **185:**3983–3988.
10. **Minamino, T., B. González-Pedrajo, K. Oosawa, K. Namba, and R. M. Macnab.** 2002. Structural properties of FliH, an ATPase regulatory component of the *Salmonella* type III flagellar export apparatus. J. Mol. Biol. **322:**281–290.
11. **Minamino, T., and R. M. Macnab.** 2000. FliH, a soluble component of the type III flagellar export apparatus of *Salmonella*, forms a complex with FliI and inhibits its ATPase activity. Mol. Microbiol. **37:**1494–1503.
12. **Minamino, T., and R. M. Macnab.** 2000. Interactions among components of the *Salmonella* flagellar export apparatus and its substrates. Mol. Microbiol. **35:**1052–1064.
13. **Minamino, T., J. R. H. Tame, K. Namba, and R. M. Macnab.** 2001. Proteolytic analysis of the FliH/FliI complex, the ATPase component of the type III flagellar export apparatus of *Salmonella.* J. Mol. Biol. **312:**1027–1036.
14. **Ohnishi, K., F. Fan, G. J. Schoenhals, M. Kihara, and R. M. Macnab.** 1997. The FliO, FliP, FliQ, and FliR proteins of *Salmonella typhimurium*: putative components for flagellar assembly. J. Bacteriol. **179:**6092–6099.
15. **Ohnishi, K., Y. Ohto, S.-I. Aizawa, R. M. Macnab, and T. Iino.** 1994. FlgD is a scaffolding protein needed for flagellar hook assembly in *Salmonella typhimurium.* J. Bacteriol. **176:**2272–2281.
16. **Ryu, J., and R. J. Hartin.** 1990. Quick transformation in *Salmonella typhimurium* LT2. BioTechniques **8:**43–44.
17. **Smyth, C. P., T. Lundbäck, D. Renzoni, G. Siligardi, R. Beavil, M. Layton, J. M. Sidebotham, J. C. D. Hinton, P. C. Driscoll, C. F. Higgins, and J. E. Ladbury.** 2000. Oligomerization of the chromatin-structuring protein H-NS. Mol. Microbiol. **36:**962–972.
18. **Toker, A. S., M. Kihara, and R. M. Macnab.** 1996. Deletion analysis of the FliM flagellar switch protein of *Salmonella typhimurium.* J. Bacteriol. **178:** 7069–7079.

19. **Vogler, A. P., M. Homma, V. M. Irikura, and R. M. Macnab.** 1991. *Salmonella typhimurium* mutants defective in flagellar filament regrowth and sequence similarity of FliI to F_0F_1, vacuolar, and archaebacterial ATPase subunits. J. Bacteriol. **173:**3564–3572.
20. **Wolf, E., P. S. Kim, and B. Berger.** 1997. MultiCoil: a program for predicting two- and three-stranded coiled coils. Protein Sci. **6:**1179–1189.
21. **Yamaguchi, S., H. Fujita, K. Sugata, T. Taira, and T. Iino.** 1984. Genetic analysis of *H2*, the structural gene for phase-2 flagellin in *Salmonella.* J. Gen. Microbiol. **130:**255–265.
22. **Zhu, K., B. González-Pedrajo, and R. M. Macnab.** 2002. Interactions among membrane and soluble components of the flagellar export apparatus of *Salmonella.* Biochemistry **41:**9516–9524.